Arch. Metall. Mater. **71** (2026), 2, 489-495

DOI: https://doi.org/10.24425/amm.2026.158828

NURUL AIDA HUSNA MOHD MAHAYUDDIN[1], JUYANA A. WAHAB[1,2,3*], MOHD ARIF ANUAR MOHD SALLEH[1,2],
MUHAMMAD FIRDAUS MOHD NAZERI[1,2,3], DEWI SURIYANI CHE HALIN[1,2]

SUBSTRATE PATTERNING EFFECT ON THE WETTING BEHAVIOUR AND INTERMETALLIC FORMATION OF SnCu ALLOY

This paper explains the effect of a micro-patterned substrate fabricated via photolithography on soldering applications. The dimple micro-pattern was fabricated on the copper substrate with a 100-500 μm diameter with a fixed depth of 25±2 μm. The dimple micro-pattern substrate was metallurgically joined with Sn-0.7Cu lead-free solder in the reflow process. The dimple micro-pattern was examined using an optical microscope (OM) to observe all the critical parameters of the photolithography. The depth of the dimple(s) was observed and measured using a 3D surface profiler. The solder joints of the dimple micro-patterned substrate and the Sn-0.7Cu solder alloy were analysed in terms of their solderability, wettability, formation of intermetallic compounds (IMCs), and microstructures to determine the influence of dimple micro-patterning on the performance of the Sn-0.7Cu solder alloy. It was observed that a fixed depth of 25±2 μm was achieved for all dimple diameters at an etching time of 45 minutes. In terms of the performance of Sn-0.7Cu solder alloy on a micro-patterned substrate, it can be seen that as the diameter of the dimples increases, the flow rate and spreading area increase. At the same time, the IMC thickness decreased as the dimple's diameter increased. The dimple micro-pattern substrate enhances copper diffusion, which reduces the β-Sn area and promotes Cu-Sn intermetallic formation, resulting in a rich, fine eutectic area of solder compared to its non-patterned counterpart.

Keywords: Surface Texture; Dimple; Micro-Pattern; Photolithography; Lead-Free Solder; Sn-0.7Cu; Wettability

1. Introduction

Previously, in the electric and electronic industry, Pb-based solders have been widely used due to their good wettability, mechanical properties, and low melting points, especially in assembling electronic circuits. However, the European Union (EU) has begun to take action by banning the use of lead in electrical and electronic products through the adoption of two directives, which require the removal of Pb from any end-of-life electrical or electronic components. The Restriction of Hazardous Substances (RoHS) banned the use of lead in all electric and electronic components manufactured since July 1, 2006. The EU Mandates by WEEE and RoHS have driven many electronic industries to migrate toward Pb-free solder due to the toxicity of lead solder alloys [1]. However, Pb-free solder alloys have poorer wetting characteristics than tin (Sn)-Pb solders, which increases the risk of solder defects. To improve the properties of Pb-free solder alloys, various types of research have been conducted to enhance their composition, including copper (Cu), silver (Ag), bismuth (Bi), nickel (Ni), and antimony (Sb). One promising method is modifying the substrate surface to achieve better solder joints [2-3].

Surface texturing is a surface modification technique that intentionally alters the surface texture [4], resulting in an improvement in the performance of the mechanical components [5]. Various technologies are applied to modify the surface characteristics in accordance with specific applications. The surface modification of the solder substrate to improve the properties of lead-free solder alloys was done by several methods, such as surface peening, laser surface texturing (LST) [6-9], lithography [10-12], electrochemical machining and wet chemical etching. One method that suits soldering applications is the use of photolithography. Photolithography is a method for producing various texture patterns on substrate surfaces using UV light.

---

[1] UNIVERSITI MALAYSIA PERLIS (UNIMAP), DEPARTMENT OF MATERIALS, FACULTY OF CHEMICAL ENGINEERING AND TECHNOLOGY, KOMPLEKS PUSAT PENGAJIAN JEJAWI 3, KAWASAN PERINDUSTRIAN JEJAWI, ARAU 02600, MALAYSIA

[2] UNIVERSITI MALAYSIA PERLIS (UNIMAP), CENTRE OF EXCELLENT GEOPOLYMER AND GREEN TECHNOLOGY (CEGEOGTECH), KOMPLEKS PUSAT PENGAJIAN JEJAWI 3, KAWASAN PERINDUSTRIAN JEJAWI, 02600, ARAU, PERLIS, MALAYSIA

[3] UNIVERSITI MALAYSIA PERLIS (UNIMAP), SURFACE TECHNOLOGY SPECIAL INTEREST GROUP, FACULTY OF CHEMICAL ENGINEERING AND TECHNOLOGY, 02600, ARAU, PERLIS, MALAYSIA

[*] Corresponding author: juyana@unimap.edu.my

Surface-modified substrates with micro-patterns, such as dimples fabricated through photolithography, are promising for electronic packaging applications, enhancing the wettability and solderability of lead-free solders. It is believed that the surface roughness of the micro-patterned copper substrate influenced the fluidity behaviours of the molten solder [13].

The steps in photolithography fabrication methods significantly influence the fabrication of micro-patterns on the copper substrate, and the effectiveness of dimple micro-pattern fabricated via photolithography on the copper substrate for lead-free solders such as Sn-0.7Cu is yet to be thoroughly reported. Therefore, this study aims to present the performance of the dimple micro-pattern that is controlled in the photolithography step. The effect of surface texturing of the copper substrate on the wettability of lead-free solder will be analysed to enlarge its potential application in electronic packaging.

2. Experiment

A high-purity copper plate (99.9%) with dimensions of 15 mm × 15 mm × 1 mm was employed as the substrate in this study, while Sn-0.7Cu served as the lead-free solder material. Dimple micro-patterns were fabricated on the copper surface using a standard photolithography technique. Prior to patterning, the copper substrates were mechanically ground and polished to achieve a smooth and scratch-free finish.

The photolithographic process involved several sequential steps: photoresist application via spin coating, soft baking, ultraviolet (UV) exposure, development, chemical etching, and photoresist removal. The design of the dimple micro-patterns with various diameters was created using AutoCAD and transferred to the substrate through a photomask. The pattern formation was governed by the masked regions during UV exposure. For coating, 2 mL of positive photoresist was applied and spin-coated at 850 rpm for 15 seconds, followed by 3000 rpm for 30 seconds, then held for 15 seconds before soft baking at 90°C for 90 seconds. The sample was then exposed to UV light using a mask aligner for 120 seconds. Subsequent development using RD-6 developer for 100-120 seconds removed unexposed photoresist, allowing pattern transfer onto the copper substrate. Etching was performed using ferric chloride ($FeCl_3$) as the chemical etchant to selectively remove unprotected copper, forming a dimple pattern with an average depth of 25±2 µm. The etching depth was dependent on the duration and pattern design. A hard bake was conducted at 90°C for 60 s to stabilise the patterns. The resulting micro-patterns were analysed using an optical microscope (OM) for morphological characterisation and a 3D profiler to quantify the dimple depths. TABLE 1 lists the sample parameters and codes.

The Sn-0.7Cu solder alloy was prepared using the conventional casting technique. A 0.4 g solder ball was placed on each dimple micro-patterned sample and reflowed in an oven with the aid of a small amount of mildly activated (RMA) flux. A non-patterned copper substrate was used as a control to assess the impact of surface patterning on solder behaviour. The spreading behaviour of the solder was visually examined and quantitatively assessed using ImageJ software. For microstructural analysis, all samples were mounted in epoxy resin and then subjected to standard grinding and polishing procedures. Cross-sectional samples were observed using an optical microscope (OM), and the contact angles between the solder and both patterned and non-patterned substrates were measured using ImageJ. The intermetallic compound (IMC) layer formed at the solder-substrate interface was also evaluated in terms of thickness and morphology. The patterned samples were compared against non-patterned substrates to evaluate the effect of surface micro-patterning on solderability performance.

TABLE 1

Dimple micro-pattern parameters

Dimple Features	**Samples**				
	T_{D100}	**T_{D200}**	**T_{D300}**	**T_{D400}**	**T_{D500}**
Diameter (µm)	100	200	300	400	500
Distance (µm)	300				
Depth (µm)	25 ± 2				

3. Results and discussion

3.1. Surface morphology of the dimple micro-pattern

The specification inspection for the micro-patterned surface was conducted to observe the critical parameters of the photolithography process, ensuring adequate development of the micro-pattern was achieved. Micro-patterns on the copper substrate need to align precisely to ensure that no defects are transferred to the micro-patterns. Therefore, any misalignment, critical dimensions, and surface irregularities, such as scratches, pinholes, stains, contamination, and effects, were observed during the dimple micro-pattern fabrication process. Fig. 1 depicts the optical image and the dimple profile of all copper substrate samples.

Optical microscopy analysis confirmed that all dimple micro-patterns were uniformly and precisely aligned on the copper substrates. Dimples fabricated under conditions T_{D100} to T_{D500} exhibited consistently circular geometries. Among them, T_{D500} required the longest average etching time, approximately 45 minutes to attain a dimple depth of 25±2 µm. In contrast, T_{D100} demonstrated the shortest average etching time, reduced by 66.67% relative to T_{D500}. As the dimple diameter decreased from T_{D500} to T_{D200}, etching times progressively decreased, with T_{D200}, T_{D300}, and T_{D400} requiring 25, 30, and 38 minutes, respectively, corresponding to reductions of approximately 44.45%, 33.33%, and 15.55%. These variations are attributed to the smaller etching area in samples with smaller dimple patterns.

Overall, the photolithography process proved highly effective for fabricating precise and well-defined micro-patterns. Its high resolution enabled the formation of sharp, scalable, and geometrically accurate features across a range of dimple sizes on the copper substrate.

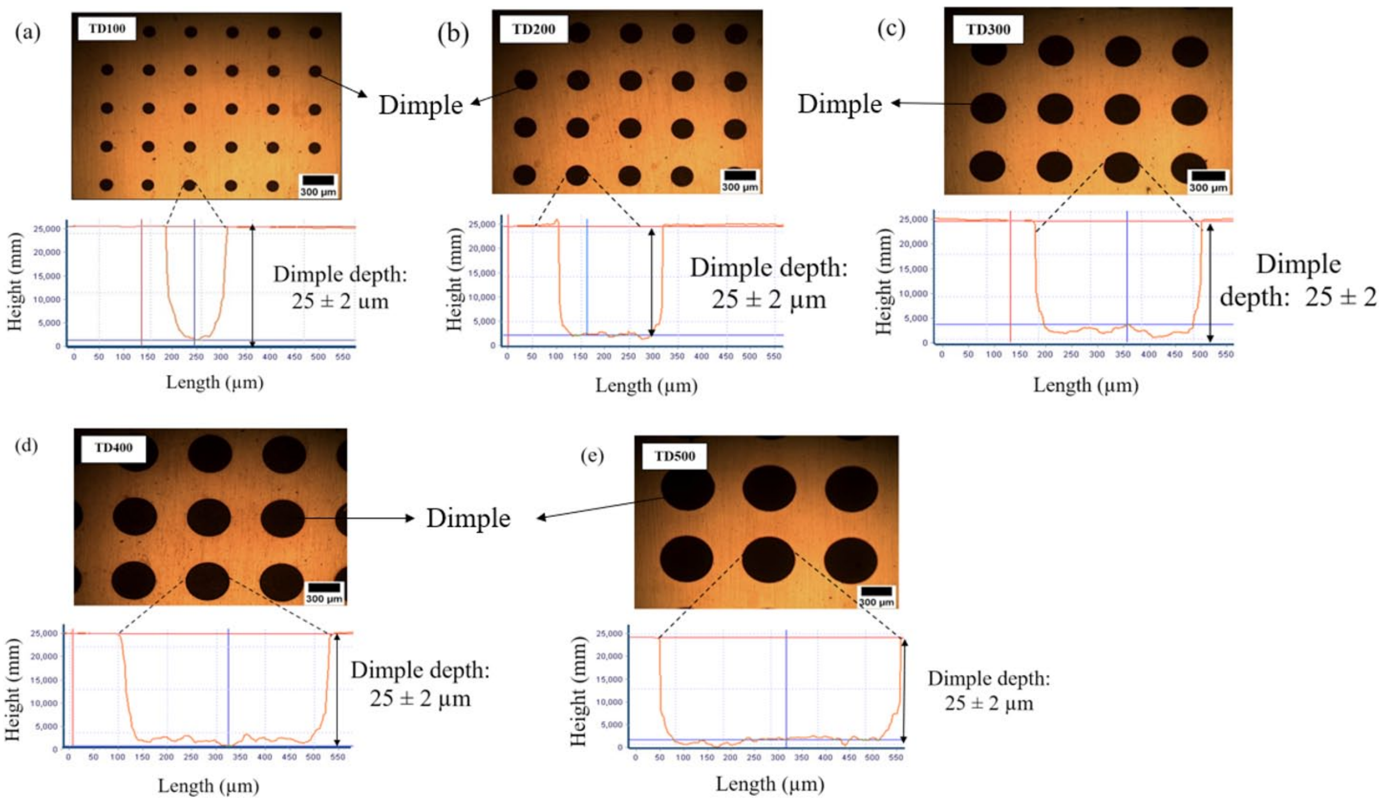

Fig. 1. Optical images and profiles of dimple micro-textured copper substrate, (a) T_{D100}, (b) T_{D200}, (c) T_{D300}, (d) T_{D400}, and (e) T_{D500}

3.2. Spreading and wetting of Sn-0.7Cu on patterned copper substrate

Fig. 2 presents the macroscopic images, spreading area and flow rate of solidified Sn-0.7Cu solder on both non-patterned and micro-patterned copper substrates. Quantitative analysis was performed to evaluate the spreading area and average flow rate of molten solder across the different substrate surfaces. The findings reveal that the introduction of dimple micro-patterns on the copper substrate significantly influences the wetting behaviour of the solder. Specifically, the incorporation of micro-patterns led to an overall increase in both the average flow rate and spreading area of the solder when compared to the non-patterned substrate. However, as the dimple diameter increased, both the flow rate and spreading area showed a declining trend, likely due to increased flow resistance caused by the patterned topography.

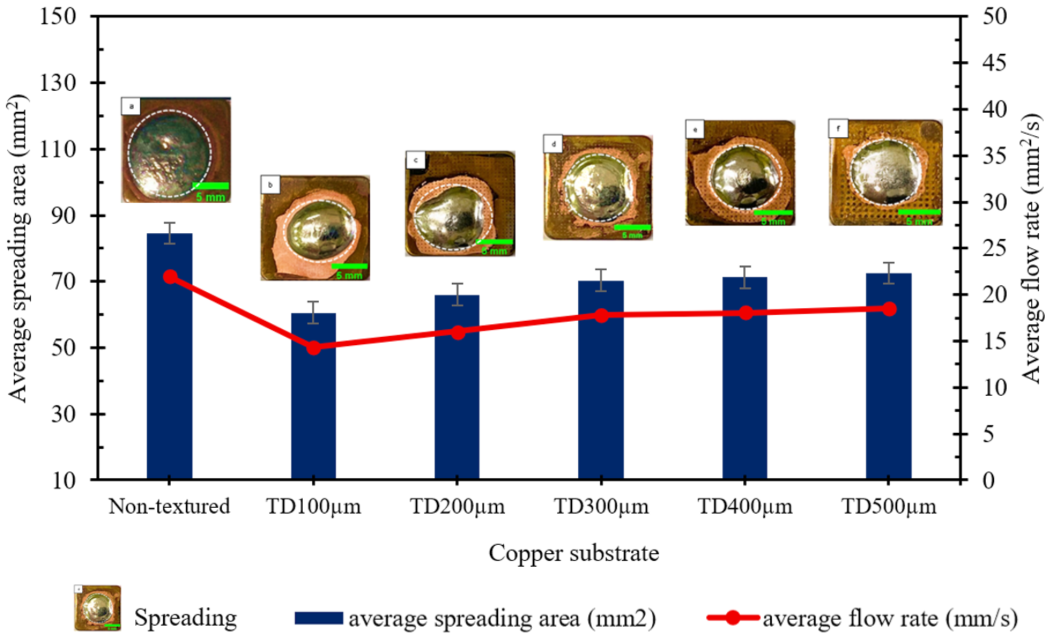

Fig. 2. Microscopic images, spreading area and flow rate of solder

Notably, the T_{D500} sample exhibited the largest dimple diameter among the patterned substrates and demonstrated a relatively high flow rate and spreading area, approaching the values observed for the non-patterned surface. This behaviour may be attributed to the reduced surface resistance and the near-equivalence in effective surface openness between T_{D500} and the flat substrate.

A higher driving force is generally required to facilitate solder spreading over patterned surfaces within a given timeframe. Among all tested samples, the non-patterned substrate exhibited the highest average flow rate (21.96 mm^2/s), facilitated by its smooth surface, which enabled unimpeded spreading of molten solder. These observations align with the findings of Satyanarayan et al. [14], who reported that surface roughness critically affects wetting behaviour by altering the interfacial area available for liquid spreading. In contrast, the dimple-patterned substrates showed lower flow rates, attributed to the microstructures impeding lateral solder movement. The entrapment of molten solder within the dimples suggests a wetting regime consistent with the Wenzel state, resulting in reduced spreading areas.

The contact angle is defined as the angle formed between the tangent at the triple-phase boundary (solid-liquid-vapor) and the solid substrate surface, serving as a key indicator of the wettability of molten solder. Fig. 3 illustrates the contact angle (θ) measurements of Sn-0.7Cu solder on both non-patterned and dimple micro-patterned copper substrates. A significant reduction in contact angle was observed for the dimpled surfaces compared to the non-patterned substrate, indicating enhanced wettability induced by surface texturing.

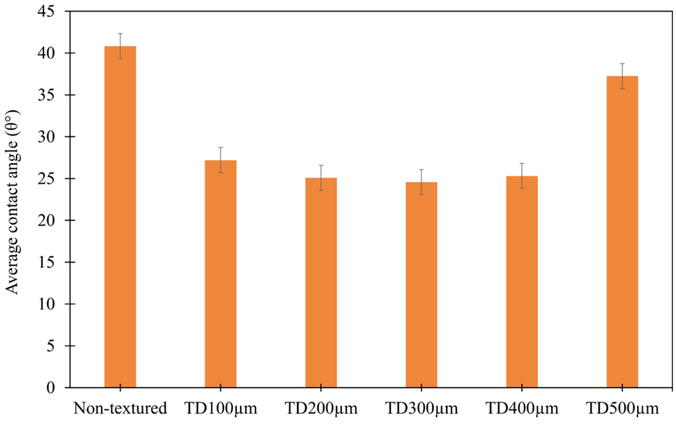

Fig. 3 Average solder's contact angle (θ°)

The non-patterned copper substrate exhibited the highest contact angle, measured at 40.8°, reflecting relatively poor wetting. In contrast, substrates patterned with dimple arrays ranging from T_{D100} µm to T_{D400} µm exhibited substantially lower contact angles, ranging from 24° to 27°. This reduction is attributed to the capillary action and entrapment of molten solder within the micro-dimples, consistent with the Wenzel wetting regime [15]. According to the Wenzel model, increased surface roughness enhances the actual contact area between the liquid and the solid, thereby promoting improved wettability.

The introduction of micro-patterned features modifies the surface topography and amplifies surface energy effects, thereby reducing the contact angle, as reported by prior findings [16]. Kubiak et al. [17] similarly reported that minor increases in surface roughness can significantly enhance wetting behaviour. Notably, the T_{D500} substrate exhibited a higher contact angle of 37.3°, which approaches that of the non-patterned substrate. This is likely due to its relatively large dimple diameter, which minimises the topographical influence on wetting behaviour, resulting in reduced enhancement of solder spreading.

3.3. Formation of the intermetallic compound

The shear strength and reliability of solder joints are largely governed by the thickness of the intermetallic compound (IMC) layer formed at the solder/substrate interface, which reflects the extent of interfacial reactions between the molten solder and the base metal [18]. While a well-formed IMC layer is essential for metallurgical bonding, excessive IMC growth can compromise joint reliability due to the inherent brittleness of these compounds [19-20].

Fig. 4 displays the morphology of the IMC layer formed at the interface between Sn-0.7Cu solder and both non-patterned and micro-patterned copper substrates. The corresponding average IMC thicknesses are presented in the bar chart in Fig. 5. It was observed that dimple-patterned substrates consistently exhibited thicker IMC layers than the non-patterned surface, with a progressive increase in IMC thickness from T_{D100} to T_{D500}. Among all samples, the T_{D500} substrate recorded the greatest average IMC thickness of 3.78 µm, while T_{D100} exhibited the lowest at 2.89 µm.

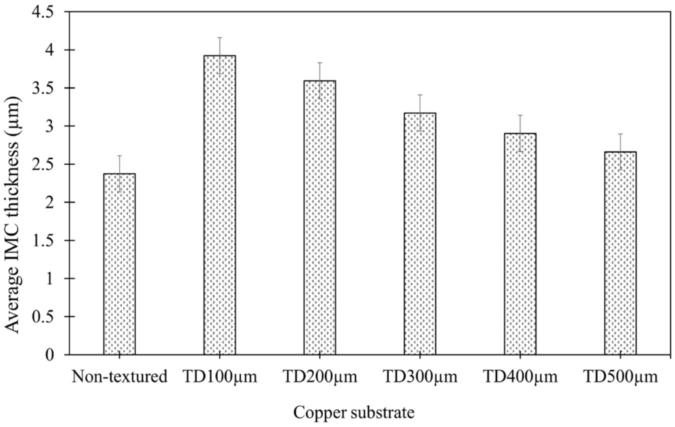

Fig. 4. Morphology of IMC layer formed on (a) non-textured substrate, (b) $T_{D100\mu m}$, (c) $T_{D200\mu m}$, (d) T_{D300}, (e) T_{D400}, and (f) T_{D500}

The increase in IMC thickness on micro-patterned substrates is attributed to the enhanced effective surface area provided by the dimple structures. These patterns facilitate a greater diffusion interface for copper atoms, as illustrated in Fig. 6. During soldering, molten Sn-0.7Cu wets the copper substrate, initiating interfacial reactions that form a Cu-Sn IMC layer. The

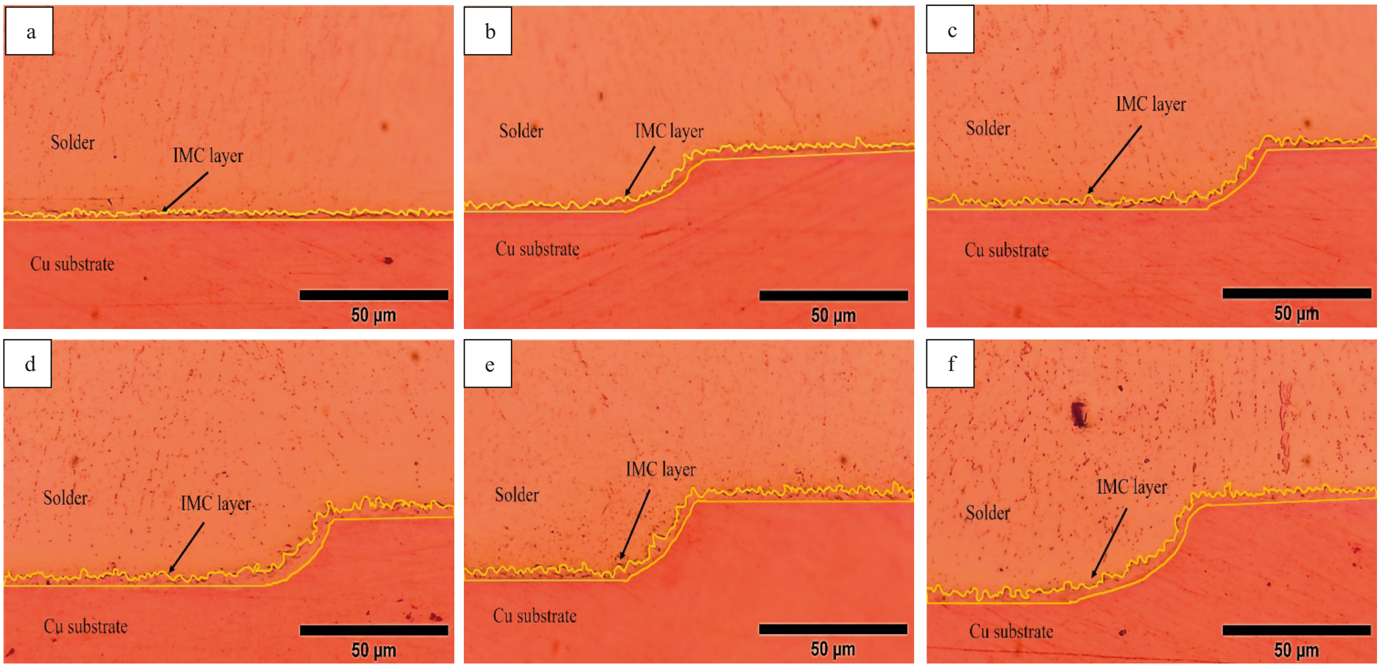

Fig. 5. Average thickness of the IMC in the solder

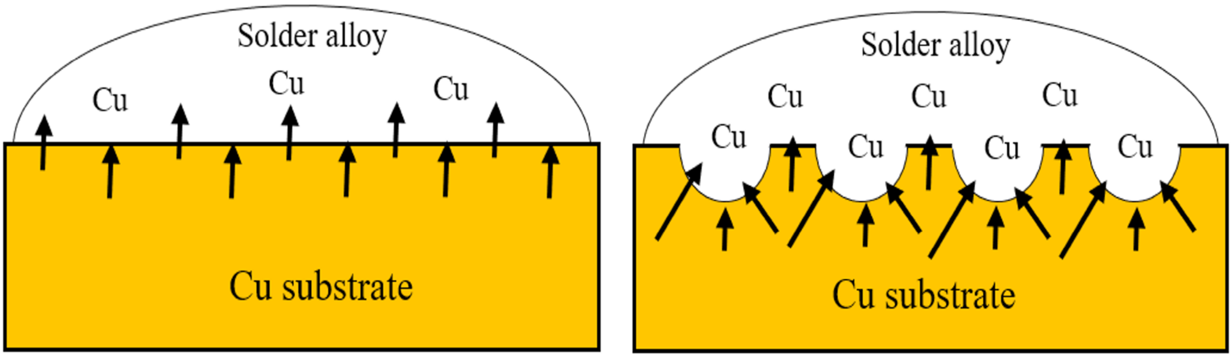

Fig. 6. Schematic illustration of copper diffusion on non-textured and textured copper substrate

diffusion of copper from the substrate and tin from the solder continues until the system reaches supersaturation [20]. This extended diffusion path, due to the increased surface topography, promotes greater IMC formation.

Although an increase in IMC thickness generally correlates with reduced mechanical integrity, particularly when the IMC exceeds a critical thickness (~10 µm), all observed IMC layers remained below this threshold. The dimple-patterned substrates showed elevated IMC thicknesses compared to the non-patterned surface; however, none exceeded the range associated with joint failure, suggesting that the enhanced interfacial area does not compromise joint reliability within the studied parameters.

Fig. 7 shows the microstructure of the bulk Sn-0.7Cu on a non-patterned and dimple micro-patterned copper substrate. The microstructure of the solidified eutectic Sn-0.7Cu bulk solder consists of two regions; Sn-rich dendrites β-Sn and eutectic region (Sn + Cu_6Sn_5) [20]. The melting process of casting Sn-0.7Cu solder bulk resulted in the formation of the eutectic phase. The morphology features of the IMC formed between the Sn0.7Cu solder and non-patterned copper substrate differed from those of the IMC formed between the Sn0.7Cu solder and patterned copper substrate. The patterned surfaces in Fig. 7(b) to Fig. 7(f), when compared, show a massive region of white dendrites relative to (a), which is a region rich in fine eutectics. The increasing amount of copper diffused from $T_{D100\mu m}$ to $T_{D500\mu m}$ reduces the β-Sn area and increases the Cu-Sn intermetallic formation, resulting in a rich fine eutectic area in $T_{D500\mu m}$ compared to $T_{D100\mu m}$. The grain size of the β-Sn-rich area of the solder was believed to be refined by copper, as Cu reacts with Sn to form Cu_6Sn_5 IMC particles, acting as heterogeneous nucleation sites during the solidification process [20].

4. Conclusions

This study presents the fabrication of dimple micro-patterns on high-purity copper substrates (99.9%) via a photolithography-based approach. Successful formation of micro-patterns required precise process control, particularly during the development and etching stages. A consistent dimple depth of 25±2 µm was

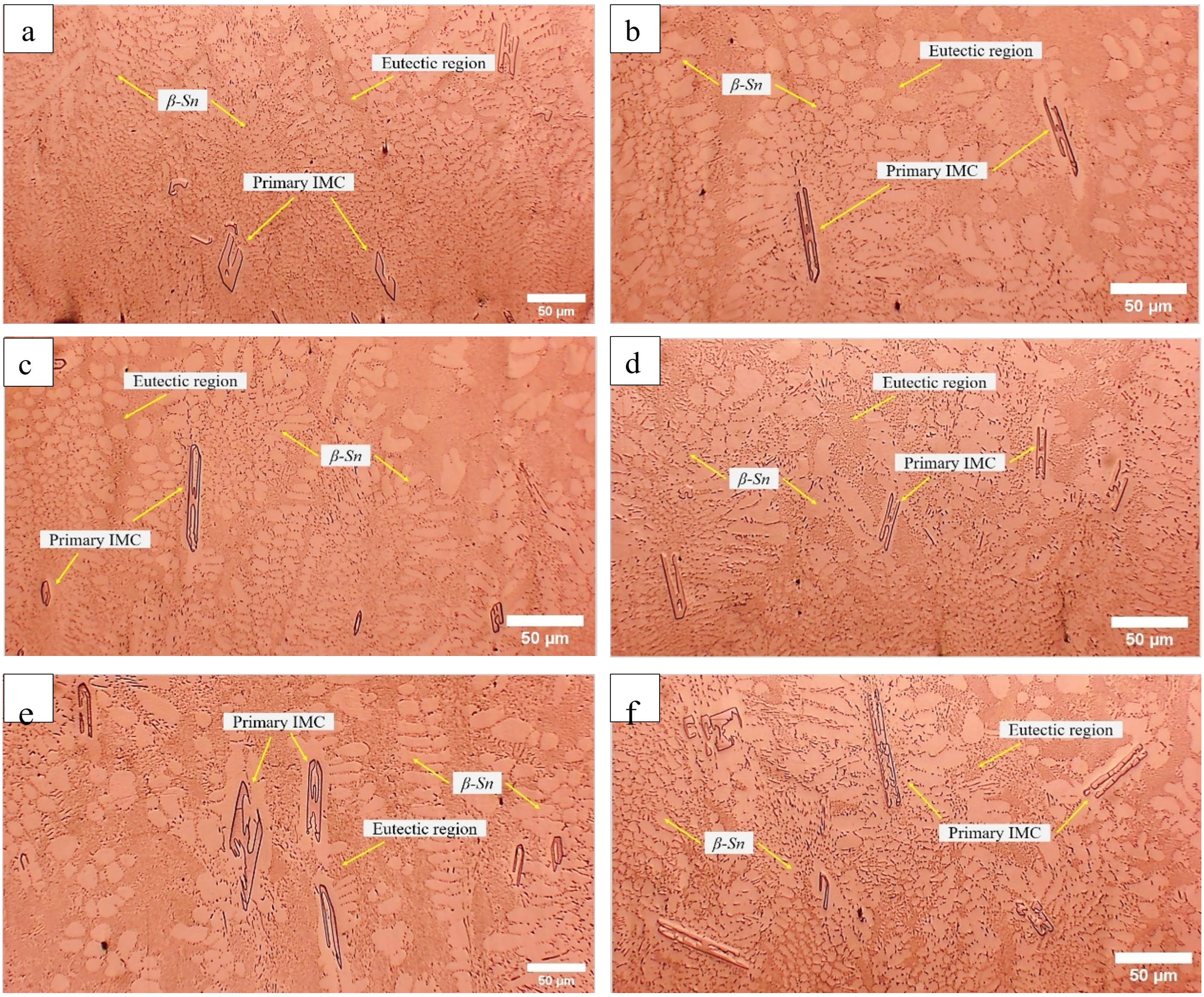

Fig. 7. Microstructure of the bulk Sn-0.7Cu on (a) non-textured substrate, (b) $T_{D100\mu m}$, (c) $T_{D200\mu m}$, (d) T_{D300}, (e) T_{D400}, and (f) T_{D500}

achieved following 45 minutes of etching. Dimple-patterned samples with varying diameters (T_{D100}-T_{D400}) exhibited reduced spreading areas and slower molten solder flow rates compared to the non-patterned substrate during reflow. In contrast, the T_{D500} sample demonstrated a significantly larger spreading area and enhanced solder flow rate, attributable to its larger dimple size, which closely resembles that of the non-patterned surface. Furthermore, patterned substrates showed lower average contact angles than the non-patterned copper, indicating improved wettability. The introduction of micro-patterns also promoted greater interfacial diffusion of copper into the solder, resulting in thicker intermetallic compound (IMC) layers. Microstructural analysis revealed dendritic formations in the T_{D100} region, while the T_{D500} sample featured a microstructure enriched with fine eutectics. In short, as the conclusion, the implementation of dimple micro-patterns on copper substrates via photolithography enhances the solderability of Sn-0.7Cu lead-free solder, offering improved wetting behaviour, solder flow, and interfacial microstructure characteristics.

Acknowledgments

The authors would like to gratefully acknowledge the financial support provided by the Fundamental Research Grant Scheme (FRGS/1/2019/TK05/UNIMAP/03/3), which is funded by the Malaysian Ministry of Education (MOE). The authors also want to thank the Materials Department, Universiti Malaysia Perlis (UniMAP) and Nihon Superior Co. Ltd. for providing guidance and support in terms of facilities during this research endeavour.

REFERENCES

[1] N.A. Saleh, M.I.I. Ramli, M.A.A. Mohd Salleh, Effect of Zinc Additions on Sn-0.7Cu-0.05Ni Lead-Free Solder Alloy. IOP Conference Series: Materials Science & Engineering **238**, 01201 (2017).

[2] H. Gao, et al., Biomimetic metal surfaces inspired by lotus and reed leaves for manipulation of microdroplets or fluids. Applied Surface Science **519**, 146052 (2020).

[3] N.S.M. Zaimi, M.A.A. M Salleh, M.M.A.B. Abdullah, M.I.I. Ramli, A Short Review on the Influence of Antimony Addition to the Microstructure and Thermal Properties of Lead-Free Solder Alloy. Arch. Metall. Mater. **68**, 3, 981-986 (2023).

[4] D.-G. Lee, Y.-J Kim, Effects of biomimetic riblet configurations on the drag reduction. DEStech Transactions on Environment, Energy and Earth Science 1-5 (2017).

[5] L. Zhang, et al., Super-hydrophobicity and corrosion resistance of laser surface textured AISI 304 stainless steel decorated with Hexadecyltrimethoxysilane (HDTMS). Optics and Laser Technology **127**, 106146 (2020).

[6] H. Yu, H. Deng, W. Huang, X. Wang, The effect of dimple shapes on friction of parallel surfaces. Journal of Engineering Tribology **225**, 693-703 (2015).

[7] J. Zhang, J. Zhang, A. Rosenkranz, N. Suzuki, E. Shamoto, Frictional properties of surface textures fabricated on hardened steel by elliptical vibration diamond cutting. Precision Engineering **59**, 66-72 (2019).

[8] J. Hu, H. Xu, Friction and wear behavior analysis of the stainless steel surface fabricated by laser texturing underwater. Tribology International **102**, 371-377 (2016).

[9] Y.Y. Chen, J.G. Duh, B.S. Chiou, Effect of substrate surface roughness on the wettability of Sn-Bi solders. Journal of Materials Science: Materials in Electronics **11** (4), 279-283 (2000).

[10] J.I. Ahuir-Torres, M.A. Arenas, W. Perrie, G. Dearden, J. de Damborenea, Surface texturing of aluminium alloy AA2024-T3 by picosecond laser: Effect on wettability and corrosion properties. Surface and Coatings Technology **321**, 279-291 (2017).

[11] H. Yue, et al., Effect of surface texturing on tribological performance of sliding guideway under boundary lubrication. Journal of Manufacturing Processes **47**, 172-182 (2019).

[12] S.J. Won, H.S. Kim, Effects of laser parameters on morphological change and surface properties of aluminum alloy in masked laser surface texturing. Journal of Manufacturing Processes **48**, 260-269 (2019).

[13] P. Pou, et al., Laser texturing of stainless steel under different processing atmospheres: From superhydrophilic to superhydrophobic surfaces. Applied Surface Science, 475 (2019).

[14] V. Satyanarayan, K.N. Prabhu, Reactive wetting, evolution of interfacial and bulk IMCs and their effect on mechanical properties of eutectic Sn-Cu solder alloy. Advances in Colloid and Interface Science **166** (1-2), 87-118 (2011).

[15] Mohammad Rezaei, David M. Warsinger, John H. Lienhard V, Mikel C. Duke, Takeshi Matsuura, Wolfgang M. Samhaber, Wetting phenomena in membrane distillation: Mechanisms, reversal, and prevention. Water Research **139**, 329-352 (2018).

[16] J. Wang, et al., Surface structure determines dynamic wetting. Scientific Reports **5**, 8474 (2014).

[17] K.J. Kubiak, M.C.T. Wilson, T.G. Mathia, P. dan Carval, Wettability versus roughness of engineering surfaces. Wear **271** (3-4), 523-528 (2011).

[18] M.A.A. Mohd Salleh, A.M. Mustafa Al Bakri, H. Kamarudin, M. Bnhussain, M.H. Zan Hazizi, F. Somidin, Solderability of Sn-0.7Cu/Si_3N_4 lead-free composite solder on Cu-substrate. Physics Procedia **22**, 299-304 (2011).

[19] G. Zeng, S. Xue, L. Zhang, L. Gao, Recent advances on Sn-Cu solders with alloying elements: Review. Journal of Materials Science: Materials in Electronics **22** (6), 565-578 (2011).

[20] R.M. Said, F.H. Mohamad Johari, M.A.A. Mohd Salleh, A.V. Sandu, The effect of copper addition on the properties of Sn-0.7Cu solder paste. IOP Conference Series: Materials Science and Engineering **318** (1), (2018).